Phys Chem Minerals (1998) 25:378–388

ORIGINAL PAPER

E. De Grave · A. Van Alboom · S.G. Eeckhout

Electronic and magnetic properties of a natural aegirine as observed from its Mössbauer spectra

Received: 26 September 1996 / Revised, accepted: 15 November 1997

Abstract A natural sample of aegirine, ideally $NaFeSi_2O_6$, has been studied by transmission Mössbauer spectroscopy in the range 4.2–480 K. At selected temperatures, a longitudinal external field of 60 kOe was applied to the absorber. The sample was observed to order magnetically at 11±1 K. The paramagnetic Mössbauer spectra (MS) show the presence of ~10% Fe^{2+} in the M1 sites of the clinopyroxene structure. These MS have been decomposed into four quadrupole doublets: two minor ones for Fe^{2+} on M1 sites, a dominant one due to Fe^{3+} on M1 sites, and a second ferric component, with a contribution of ~3% and attributable to the tetrahedral sites. Two possibilities concerning the origin of the two distinct Fe^{2+} (M1) doublets are discussed. They are respectively based on inter-valence charge transfer and on the existence of distinct Fe^{2+} orbital configurations at the two M1 sites. Neither of the two models could be firmly excluded. The asymmetry parameter η of the electric field gradient at the Fe^{3+} (M1) sites is close to 1.0 and the quadrupole splitting within 0.34±0.01 mm/s at all temperatures. The MS at 4.2 K shows an asymmetric hyperfine-field distribution for Fe^{3+}, with a maximum-probability field of 468 kOe. The maximum-probability field for Fe^{2+} is found to be 220 kOe. The shape of the applied-field MS at 4.2 K implies a static antiferromagnetic ordering and was successfully interpreted by a bidimensional distribution of the magnitude and orientation of the hyperfine field. Finally, the temperature variations of the respective centre shifts and quadrupole splittings could be explained on the basis of existing theoretical models.

E. De Grave (✉) · A. Van Alboom[1] · S.G. Eeckhout
Department of Subatomic and Radiation Physics,
University of Gent, Proeftuinstraat 86, B-9000 Gent, Belgium
Fax No: +32-9-264.66.99
Email: eddy.degrave@rug.ac.be

Present address:
[1] High School Gent, Department Industrial Sciences,
Schoonmeersstraat 52, B-9000 Gent, Belgium

Introduction

Aegirine, $NaFeSi_2O_6$. belongs to the group of clinopyroxenes, the Na^+ cations occupying the M2 positions with eight-fold oxygen co-ordination, and the Fe^{3+} cations the octahedral M1 positions. As usual, natural samples show compositions which deviate from the ideal one, and for instance can be classified as members of the solid-solution series aegirine/hedenbergite ($CaFeSi_2O_6$), or aegirine/diopside ($CaMgSi_2O_6$). There is some controversy in the literature with respect to the nomenclature of the minerals belonging to this class of clinopyroxenes. Tröger (1952) and Deer et al. (1978) proposed to use the name aegirine for those members containing more than 0.75 ferric ions per formula unit. Other pyroxene specialists (Cameron and Papike 1980; Langer K, personal communication 1997) prefer the name acmite. Following the recommendations of the Subcommittee on Pyroxenes of the International Mineralogical Association (Morimoto 1988), aegirine will be used in this paper.

A number of Mössbauer studies on Fe-bearing clinopyroxenes have been reported in the past decades. Dollase and Gustafson (1982) examined the Mössbauer spectra (MS) recorded at 77 K and room temperature (*RT*) for a number of mixed series. The MS for the series ($NaFeSi_2O_6$) – ($CaFeSi_2O_6$) consist of a predominant Fe^{3+} doublet with quadrupole splitting ΔE_Q at *RT* increasing from 0.29 mm/s for the Na end-member, to 0.46 mm/s for the 20Na–80Ca composition. With increasing Ca content, this doublet was found to become more and more asymmetrically broadened. In addition, two weaker Fe^{2+} doublets were resolved and attributed to two distinct M1 sites. A remarkable finding was that with the increase in temperature the population of one of the Fe^{2+} sites grows at the expense of the other one. For this observation, as well as for the existence of two sites, a clear-cut explanation could not be found. Amthauer (1982) and Amthauer and Rossman (1984) found similar spectral features for a natural, Ca- and Fe^{2+}-containing aegirine. These authors interpreted the temperature variations of the two doublet ar-

eas as being the result of a thermally activated electron exchange between Fe^{2+} and Fe^{3+} on adjacent M1 sites. The slightly asymmetric broadening of their Fe^{3+} doublet reportedly indicates the appearance of relaxation effects.

Baum et al. (1988) measured a magnetically split MS for a synthetic aegirine at 2 K. They obtained a hyperfine field H_{hf} of 461 kOe, however with a tremendous broadening of the Lorentzian lines. In contrast, for a natural sample at 2 K de Oliveira et al. (1988) adjusted three sextet components with H_{hf} values in the range 424–462 kOe, all with reasonably narrow line widths.

The present work concerns a detailed study of a natural aegirine and has been undertaken in an attempt to contribute to a better insight in the Mössbauer behaviour of this mineral.

Experimental

The sample of unknown origin was provided by the Geological Museum of the University of Gent. The powder X-ray diffraction pattern shows, in addition to the reflections of aegirine (JCPDS file 18-1222), a few fairly weak diffraction lines which could not be identified. However, it was made sure that these reflections do not originate from an iron-bearing amphibole or oxide. The most intense (~3% relative to the most intense aegirine reflection) of these unwanted reflections was found at a *d*-spacing of ~0.33 nm and could therefore be due to quartz. As the amount of impurity phase is very small, it will not significantly affect the chemical and, more importantly, the Mössbauer results.

The elemental composition of the sample, as determined by energy-dispersive X-ray analysis, can be written as:

$$Na_{1.06}Ca_{0.06}Mg_{0.04}Fe_{1.01}Al_{0.06}Si_{1.91}O_6,$$

however, due to the presence of the impurity phase, this composition is only approximately correct as far as the aegirine phase is concerned. MS were collected at temperatures in the range 4.2–480 K, in steps of 20 K on average, with a conventional, constant-acceleration drive and triangular reference signal. The absorber had a thickness of approximately 10 mgFe/cm^2 and was oriented at the magic angle (≈54°) with respect to the γ-ray beam in order to avoid texture-induced asymmetry in doublets' line intensities (Nagy 1978). Counts were accumulated in 1024 channels and all spectra were run until an off-resonance count rate of at least 10^6 counts/channel (unfolded spectrum) was reached. At selected temperatures an external magnetic field of 60 kOe was applied parallel to the incident γ-ray beam. The velocity scale of the spectrometers was calibrated using the MS of standard absorbers (α-Fe or α-Fe_2O_3). The velocity increment per channel was ~0.045 mm/s (magnetically split MS) or ~0.015 mm/s (paramagnetic MS). The magnetic order-disorder transition temperature was determined by measuring the temperature variation of the transmission of γ-rays through the absorber with the source at zero velocity, the so-called thermal-scan method (Chambaere and De Grave 1984), and found to be 11±1 K, which is within the range found earlier for both synthetic (Baum et al. 1988; Ballet et al. 1989) and natural (de Oliveira et al. 1988; Ballet et al. 1989) aegirines.

Results and spectral analyses

Paramagnetic MS

Example paramagnetic MS at a few selected temperatures are shown in Fig. 1. Inspired by the shape of the high-temperature observations, all spectra have initially been fitted as a superposition of one ferric doublet (D1 in Fig. 1) and two weak ferrous doublets (D2, D3), all with Lorentzian line shapes. The latter two were assumed to be symmetrical, while the predominant Fe^{3+} component was found to possess an asymmetry $R_q \approx 0.93$ over the entire temperature range. According to some authors (Amthauer and Rossman 1984), the asymmetry of D1 is due to relaxation effects. It is indeed well established that these effects may induce asymmetrical doublets, however this feature is mostly restricted to a relatively narrow temperature range above the ordering temperature (Wickman and Wertheim 1968), while in the present case the asymmetry persists up to 480 K, and most likely higher. Therefore, it is not believed that the Fe^{3+} line shape reflects the presence of relaxation phenomena.

In a next stage, the present authors succeeded in fitting four symmetrical doublets to the observed MS, three of which yielded similar parameter values to those of D1, D2, and D3. The fourth component, D4, with fractional area of 0.03±0.01, is characterised by hyperfine parameters which could indicate a ferric state in a tetrahedral co-ordination, viz., δ=0.17 mm/s and ΔE_Q=0.17 mm/s, both at *RT*, although this latter value is considerably smaller than the quadrupole splittings commonly found for the Fe^{3+} in a number of clinopyroxenes (Akasaka 1983). The obtained goodness-of-fit values of these four-doublet fits were consistently lower by 10–20% than for the three-doublet fits. As seen from Fig. 1, in which the full lines represent the four doublets and their addition as fitted to the experimental data, the seemingly asymmetric peak depth of the major component is excellently reproduced by the introduction of the fourth doublet. For these reasons, a four-doublet model is preferred against the three-doublet one.

The Mössbauer parameters of the four doublets at some selected temperatures are listed in Table 1. On the basis of these values and of literature data (Annersten and Nyambok 1978), D1, D2, and D3 are attributable to the M1 sites. The line widths for D1 and D2 are close to 0.30 mm/s at all temperatures, while D3 exhibits a considerable line broadening, from 0.4 mm/s at 30 K up to over 1.0 mm/s at 480 K. Due to the complete overlap of D4 by D1, the line width for the former had to be constrained in order to arrive at consistently varying parameter values for this tetrahedral site. The value of the instrumental width (0.25 mm/s) was chosen. The observed variations, with temperature, in the fractional area of the D2 and D3 components, the line broadening of D3, and the unusually steep temperature dependence of its δ value, are all in line with the observations of Amthauer and Rossman (1984) who attributed these phenomena to thermally activated electron hopping.

Paramagnetic MS in an applied field

Mössbauer spectra at 80 K and 277 K in an applied field of 60 kOe are reproduced in Fig. 2. The line shape of this

Table 1 The relevant Mössbauer parameters at selected temperatures of the four doublets fitted to the spectra of aegirine. Centre shift δ (relative to α-Fe) and quadrupole splitting ΔE_Q are in mm/s. S is the fractional doublet area

T(K)	D1: Fe^{3+} (M1)			D2: Fe^{2+} (M1)			D3: Fe^{2+} (M1)			D4: Fe^{3+} (T)		
	δ	ΔE_Q	S	δ	ΔE_Q	S	δ	ΔE_Q	S	δ	ΔE_Q	S
30	0.504	0.34	0.85	1.28	3.07	0.08	1.30	2.26	0.03	0.32	0.18	0.04
80	0.500	0.35	0.85	1.27	3.07	0.07	1.27	2.27	0.04	0.29	0.16	0.04
200	0.450	0.34	0.85	1.22	2.97	0.06	1.22	1.96	0.05	0.24	0.17	0.04
298	0.384	0.34	0.87	1.14	2.77	0.05	1.08	1.87	0.05	0.17	0.17	0.03
400	0.335	0.33	0.86	1.09	2.57	0.03	1.00	1.73	0.08	0.11	0.15	0.03
480	0.285	0.33	0.85	1.04	2.34	0.02	0.95	1.29	0.10	0.10	0.10	0.03
Error	0.005	0.01	0.02	0.02	0.03	0.01	0.02	0.03	0.01	0.02	0.03	0.01

kind of MS is largely determined by the asymmetry parameter η of the electric field gradient (EFG) (Collins and Travis 1967). It is obvious that at the higher T this line shape displays better resolved features than at 80 K. This is a consequence of the field reduction due to spin polarisation. The magnitude of this reduction is proportional to the magnetic susceptibility (Johnson 1967), and hence increases with decreasing temperature. In case of Fe^{3+}, which has isotropic magnetic properties, only one field-reducing parameter, H_{red}, has to be considered. For Fe^{2+} species in a non-cubic environment, however, the field reduction is anisotropic and its magnitude thus depends on the crystallographic direction. It is then required to introduce three values, commonly denoted *HIX*, *HIY*, *HIZ* (Varret 1976a) in which X, Y, and Z refer to the principal-axes frame of the EFG. In the present study, due to the weak contributions of the ferrous doublets, this anisotropy was ignored and only the isotropic quantity H_{red} was considered.

The applied-field MS (AFMS) have been computer analysed by diagonalization of the complete hyperfine-interaction Hamiltonian (HIH), however with several constraints. Due to the lack of sufficient fine-structure at 80 K, only one ferric (D1) and one ferrous (D23) component have been considered, both with adjustable δ, ΔE_Q, η and H_{red}. The obtained results for δ and ΔE_Q of Fe^{3+} were found to be in excellent agreement with the zero-field data. The value for $\eta(Fe^{3+})$ is high, viz., 0.8, but unprecise and imposing $\eta(Fe^{3+})=1.0$ produced an equally good fit.

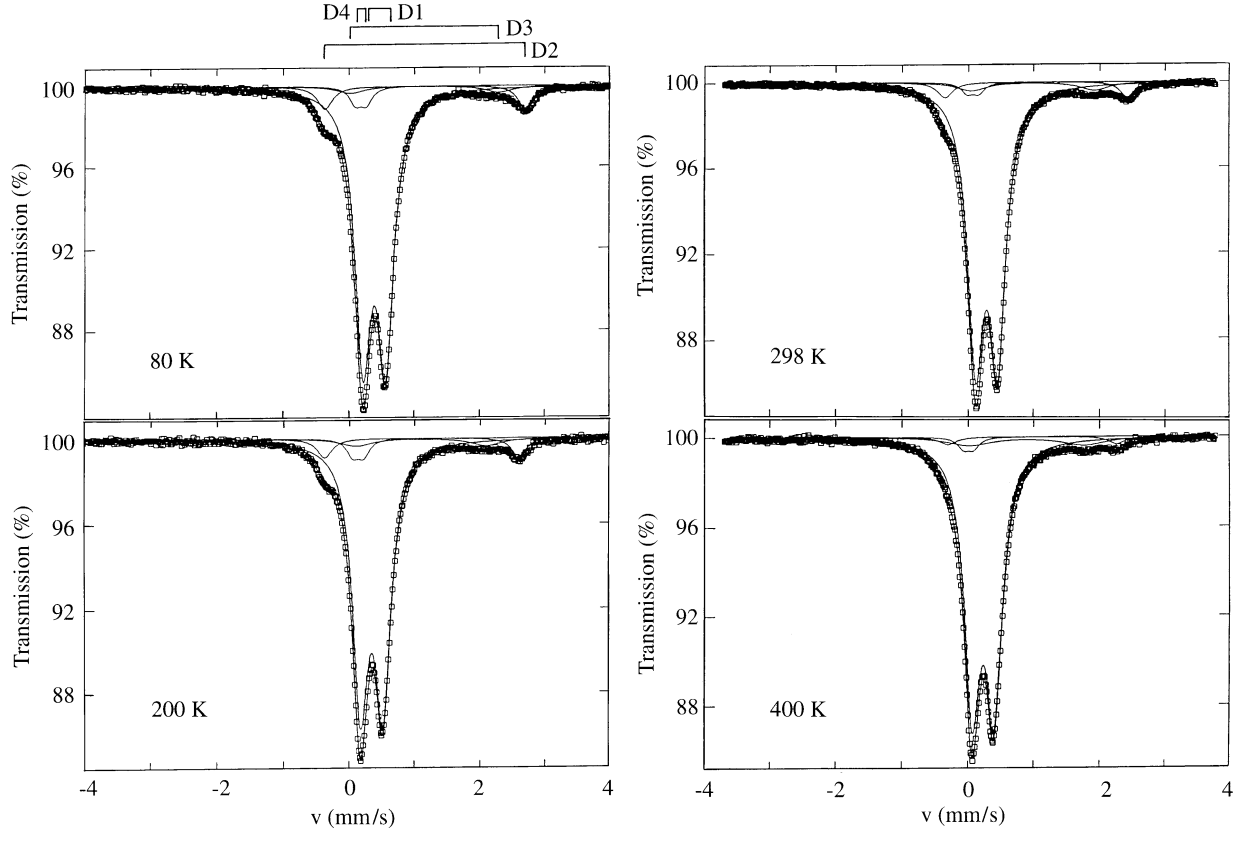

Fig. 1 Mössbauer spectra of aegirine at selected temperatures as indicated. The spectra have been decomposed into four quadrupole doublets (D1, D2, D3, D4) as shown by the full lines

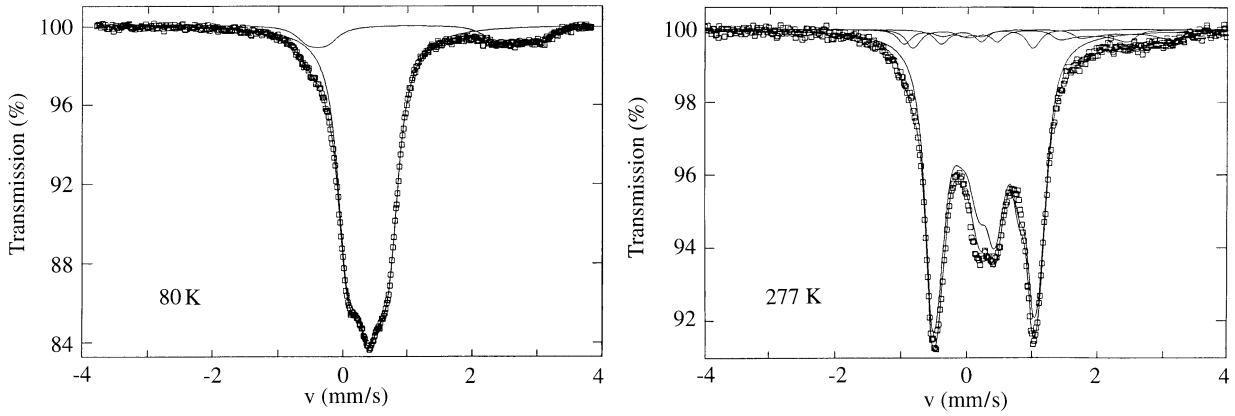

Fig. 2 Mössbauer spectra of aegirine at 80 K and 277 K with the absorber subjected to an external magnetic field of 60 kOe applied parallel to the incident γ-ray beam

As a result of this high η and of the low resolution, the sign of the principal EFG component, V_{zz}, has remained undetermined. The field reductions were found to be very high, ≈−50 kOe.

The AFMS at 277 K was fitted with four components. The values of δ and ΔE_Q for D2, D3 and D4, as well as their fractional areas S, were forced to be equal to those derived from the zero-field MS recorded at 275 K. In spite of this rather severe constraints, the observed line shape is reasonably well reproduced by the calculated one (see Fig. 2, full lines), with some minor deviations. The fitted δ and ΔE_Q values for D1 are equal, within the experimental error limits, to the zero-field data. The η value for the ferric M1 site is again high (0.85 for the fit shown in Fig. 2) and therefore the sign of V_{zz} could not be determined. Due to their weak intensities and strong overlap, it is obvious that the V_{zz} signs for the three other components have also remained undetermined. The field reduction for Fe^{3+} (M1) was fitted to be −18 kOe, which is not unreasonably high. A simple calculation leads to a reduction of ∼30% of the external-field value at 277 K, which is indeed in good agreement with the adjusted value. This estimation was based on the formula (Johnson 1967):

$$H_{red}=-H_{ext}[\chi_m H_{hf}(0)/Ng\mu_B S]$$

with H_{ext}=60 kOe, χ_m the molar susceptibility, $H_{hf}(0)$ the saturation hyperfine field (see next section) and $Ng\mu_B S$ the theoretically expected saturation magnetisation. χ_m may be estimated using the well-known Curie-Weiss law for paramagnets:

$$\chi_m=C_m/(T-\Theta_p),$$

C_m being the Curie constant and Θ_p the paramagnetic Curie temperature. These quantities were taken as 4.4 Kcm^3mol^{-1} and −39 K respectively, as determined by Baum et al. (1988) for pure synthetic aegirine $NaFeSi_2O_6$.

A major conclusion derived from these paramagnetic AFMS concerns the large magnitude of the asymmetry parameter at the Fe^{3+}(M1) sites. This finding implies that the geometry of these sites is strongly deformed from axial symmetry.

Fig. 3 Mössbauer spectrum of aegirine at 4.2 K. The spectrum has been fitted as a superposition of an Fe^{2+} and an Fe^{3+} hyperfine-field distribution (full lines). The resulting probability distributions are shown on the right, the one referring to Fe^{3+} being decomposed into six Gaussians (full lines)

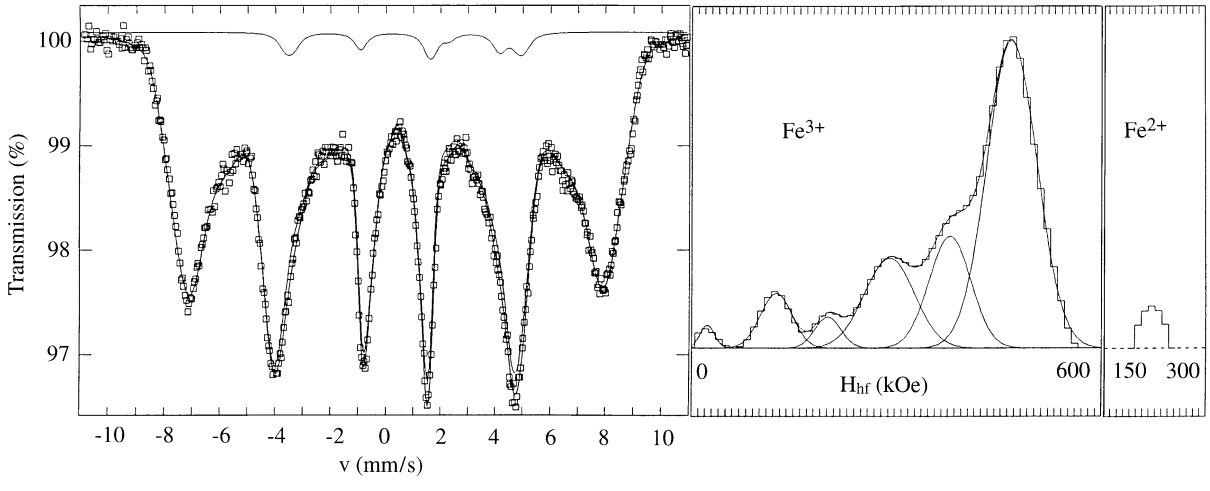

Magnetically split MS

The MS recorded at 4.2 K is depicted in Fig. 3 and is typical for a very broad distribution of hyperfine fields. It was interpreted as a superposition of two model-independent magnetic hyperfine-field distributions (MHFD), one for Fe^{3+} and one for Fe^{2+}. It was found impossible to consider four components as in the case of the paramagnetic MS. This means that the obtained quantities for Fe^{3+} will refer to the M1 sites, while those for Fe^{2+} will be average values for the two M1 sites dealt with earlier.

The computer program used for the fit was an adapted version of the nowadays routinely and widely used approach for the calculation of the MHFD from MS of ferric species (Vandenberghe et al. 1994). The field range for Fe^{3+} was between 0 and 600 kOe in steps of 10 kOe. The adjustable parameters were δ, a linear correlation between quadrupole shift, $2\,\varepsilon_Q$, and the field value, and the width of the elementary Lorentzian sextet. The linear correlation was required to account for the remaining slightly asymmetric peak depths of corresponding absorptions (see Fig. 3, lines 1 and 6, lines 2 and 5) otherwise. The distributed Fe^{2+} component was obtained from the complete HIH, the strength of the quadrupole interaction being comparable to that of the magnetic dipole interaction.

Table 2 Results of the hyperfine-field distribution fit of the 4.2 K, zero-field MS [$2\,\varepsilon_{Q,m}$ (in mm/s) is the Fe^{3+} quadrupole shift and $\Delta E_{Q,\,m}$ (in mm/s) the Fe^{2+} quadrupole splitting, both corresponding to the maximum-probability hyperfine field $H_{\mathrm{hf},\,m}$ (in kOe), and $C_{Q,\,H}$ (in mm/s.kOe) are the slopes of the linear correlations between the field and the quadrupole shift or splitting]

Pattern	δ	$2\,\varepsilon_{Q,m}$	$\Delta E_{Q,\,m}$	$H_{\mathrm{hf},\,m}$	$C_{Q,\,H}$	S
Fe^{3+}	0.48	0.03		467	–0.0005	0.95
Fe^{2+}	1.27		3.10	220	0.0014	0.05

Fig. 4 Mössbauer spectrum of aegirine at 4.2 K with the absorber subjected to an external, longitudinal field of 60 kOe. The spectrum has been analysed with a two-parameter distribution with the hyperfine field H_{hf} ranging between 0 and 600 kOe, and its orientation φ with respect to the external field ranging between 0° and 180°. The middle part presents a perspective view of the obtained ($H_{\mathrm{hf},\,\phi}$) distribution. The right part shows the integrated angle distribution

The field interval was [190–250] kOe, with steps of 10 kOe. Again, δ, a linear correlation between ΔE_Q and H_{hf} and the line width were iterated. The other hyperfine parameters appearing in the HIH have been fixed at η=0 and θ=80°. The latter quantity is the angle between the EFG's principal axis and the direction of the hyperfine field, and was chosen as such because that value was found for the M1 sites in hedenbergites (Van Alboom 1994). It has, however, very little effect on the relevant parameters obtained from the iteration. Finally, the relative spectral areas S were also adjustable.

Some results of the fitting procedure are listed in Table 2. It is clear that the Fe^{2+} parameters again are less precisely determined, especially the slope $C_{Q,\,H}$ of the linear ΔE_Q–H_{hf} relation and S. The low value for the latter is therefore undoubtedly an artefact. The slope $C_{Q,\,H}$ of the Fe^{3+} component is significant and means that the quadrupole shift decreases with increasing field strength. This is consistent with the results of de Oliveira et al. (1988), who fitted their 2 K MS by a superposition of three discrete sextets. Their results clearly show a negative correlation of $2\,\varepsilon_Q$ with H_{hf}. As mentioned in the previous section, the paramagnetic MS revealed a narrow line width for Fe^{3+} (M1), viz., ≤0.30 mm/s. This implies that the fluctuations of its quadrupole splitting ΔE_Q are minor and hence that the $2\,\varepsilon_Q$ distribution, reflected in the magnetic Fe^{3+} component, is due to static fluctuations of the above defined angle θ. It should be noted at this point that Baum et al. (1988) found from their 5 K spectrum of synthetic $NaFeSi_2O_6$ a zero quadrupole shift, in line with the present result for the Fe^{3+} (M1) site. The authors explained this observation as being a result of a geometrical change of this site on cooling down below the transition temperature. It is more likely, however, that the zero value reflects a distribution of the angle θ, the quadrupole shift being related to the quadrupole splitting by the well-known expression $2\,\varepsilon_Q = 1/2\,\Delta E_Q\,(3\cos^2\theta - 1)$. For a random θ the angle-dependent term equals zero.

The calculated H_{hf} distribution profiles are reproduced in the right part of Fig. 3. The one referring to Fe^{3+} is clearly multimodal and could be described by a superposition of six Gaussian curves (see full lines in Fig. 3). The weakest one, centred around 23 kOe, is certainly unreal and the second one at 122 kOe may be doubted as well.

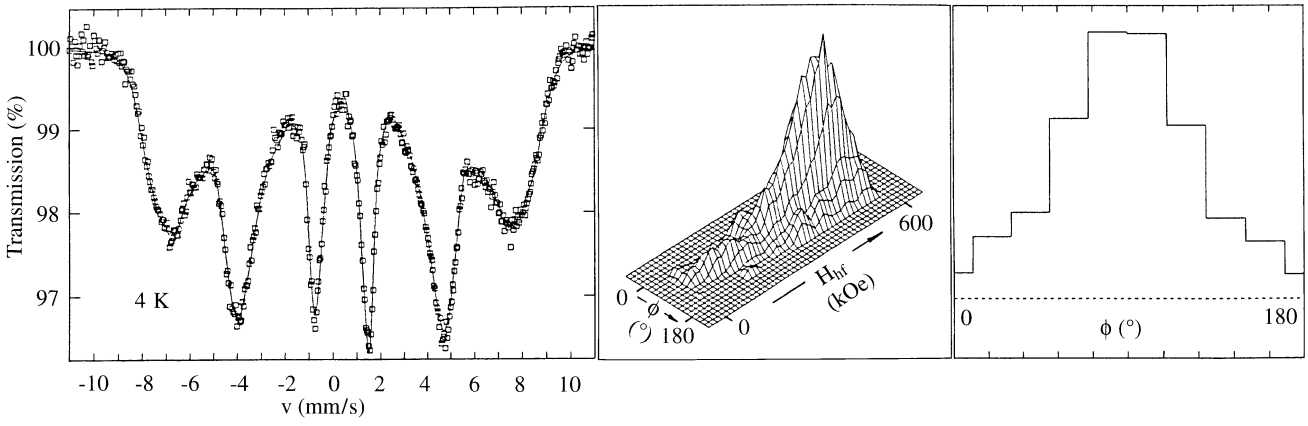

These artefacts are the result of the fitting procedure not being valid for small field values (Le Caër et al. 1984). The four remaining maxima have positions at 198, 287, 376, and 468 kOe. It is tempting to ascribe these more or less distinct fields qualitatively to different nearest-neighbour cation configurations, and consequently different magnetic-exchange interaction strengths, for the probe Fe nuclei. At reduced temperatures of $T/T_N \approx 0.4$, as for this aegirine sample at 4.2 K, such differences may lead to considerably different H_{hf} values (Sawatzky et al. 1969). At lower T/T_N values, these field values are expected to be spread-out over less broad intervals. It is interesting to note in this respect that the three distinct sextets used by de Oliveira et al. (1988) to describe their MS recorded at $T/T_N \approx 0.13$ have fields of 462, 445, and 422 kOe respectively. This is qualitatively in line with the foregoing reasoning. Considering the rather complicated composition of the investigated sample, no attempts have been undertaken to relate the calculated relative areas of the five Gaussian profiles to the probabilities of the various nearest-neighbour arrangements for a Fe^{3+} (M1) site.

The AFMS recorded at 4.2 K is shown in Fig. 4. Apart from the smaller overall splitting, the shape of this spectrum is similar to that of the zero-field MS, implying that a field strength of 60 kOe is too low to affect the spin structure, which is therefore antiferromagnetic, in agreement with earlier magnetisation measurements (Baum et al. 1988; de Oliveira et al. 1988; Ballet et al. 1989). This further means that both the magnitude of the effective hyperfine field, H_{eff}, which is the vectorial composition of the external field, and the hyperfine field, and its direction ϕ with respect to the external field, are distributed. Hence, this spectrum cannot be fitted properly using the above mentioned MHFD routine.

The two-parameter distribution procedure described by de Bakker et al. (1990) was applied to interpret the line shape of the AFMS. For the sake of simplicity and to keep computing times within reasonable limits, only one component was considered with a H_{hf} range of [0–600] kOe at steps of 15 kOe. The angle ϕ varied between 0° and 180° in steps of 18°. In addition to δ, a linear ($2\varepsilon_Q$, H_{hf}) correlation was iterated as well. The calculated spectrum is shown in Fig. 4 (full line) and reproduces the observed line shape reasonably well, despite the omission of the Fe^{2+} contribution. A three-dimensional view of the (H_{hf}, ϕ) distribution is presented in the middle part of Fig. 4. It is clear that the multimodal shape of the MHFD as obtained from the zero-field MS is reflected in the two-dimensional distribution. The different maxima in the latter, however, are less resolved, which is in part due to the broader step used to divide the total field range. The maximum-probability hyperfine field $H_{hf,m}$ was calculated to be 438±5 kOe and is significantly lower than the value derived from the zero-field MS (see Table 2). It is not believed that this discrepancy is an artefact of the fitting procedure, since good agreement between the two differently determined $H_{hf,m}$ values was found for other antiferromagnetic powders, i.e., goethite (de Bakker et al. 1990) and lepidocrocite (De Grave et al. 1992). A possible reason could be that the temperature at which the AFMS was recorded, was slightly higher than that for the zero-field measurement. Considering the low Néel temperature of the compound, a raise of 0.5 K can explain the lower field value.

The drawing on the right in Fig. 4 represents the distribution probabilities for the various ϕ values each integrated over the entire H_{hf} range. The shape of this histogram approaches that of a random distribution and the calculated value of the maximum-probability angle, viz., 89°, confirms the suggestion of a random orientation of the spins with respect to the applied-field direction. Finally, the values for δ, $2\varepsilon_{Q,m}$, and $C_{Q,H}$ were iterated as 0.49 mm/s, 0.00 mm/s, and −0.0005 mm/s.kOe respectively, all in excellent agreement with the corresponding data presented in Table 2. This finding supports the earlier discussion concerning the discrepancy between the two $H_{hf,m}$ values.

Discussion

Temperature dependence of the centre shifts

The observed centre shifts for the four Fe sites are plotted as a function of T in Fig. 5. As usual, these variations have been interpreted on the basis of the expression (Heberle 1971):

$$\delta(T)=\delta_I+\delta_{SOD}(T). \quad (1)$$

The intrinsic isomer shift δ_I is weakly dependent upon T as a result of the thermal expansion of the lattice. However, the effect of this dependence is noticeable only at temperatures exceeding the range considered in this study (De Grave and Van Alboom 1991), and therefore δ_I was treated as a constant. The second-order Doppler shift δ_{SOD} and its T dependence are determined by the lattice-vibra-

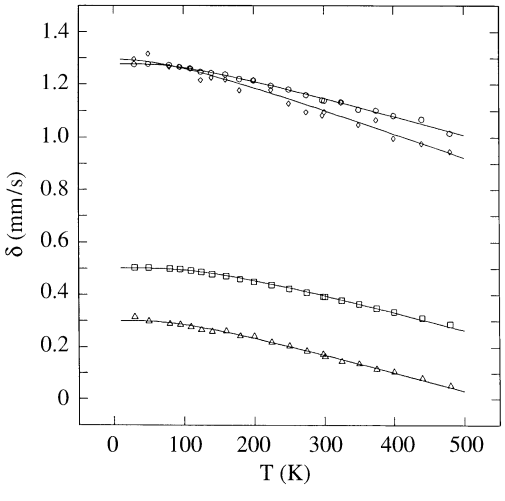

Fig. 5 Temperature variations of the centre shifts δ for the four doublets D1 (□), D2 (○), D3 (◊), and D4 (Δ) fitted to the paramagnetic spectra of aegirine. The full lines are the calculated variations assuming the Debye model for the lattice vibrations of the iron nuclei

tional spectrum and can be consistently calculated using the Debye approximation for this latter spectrum (De Grave and Van Alboom 1991). Such a calculation produces a value for the so-called characteristic Mössbauer or lattice temperature, Θ_M. The method was found to give consistent results for Fe^{3+} (M1) and D2-Fe^{2+} (M1), with Θ_M=540 K, δ_I=0.64 mm/s and Θ_M=380 K, δ_I=1.38 mm/s respectively, yielding the full lines (Fig. 5) for the theoretical variations with T. The values for Θ_M are in excellent agreement with the range of values that are typical for ferric and ferrous ions in six-fold oxygen co-ordinations for a large variety of synthetic and natural compounds (De Grave and Van Alboom 1991). The Mössbauer fractions f_3 and f_2 at 80 K, calculated from these Θ_M values, are 0.93 and 0.89 for Fe^{3+} (M1) and D2-Fe^{2+} (M1) respectively. At 480 K, both have decreased to 0.79 and 0.63 respectively.

For Fe^{3+} (T) it was found that Θ_M=380 K, which is unacceptably low since it is experienced that in a given compound the co-ordination has but a small, sometimes insignificant, effect on the magnitude of this quantity. The reason for this shortcoming is the not so precise determination of the δ values as a result of the doublet D4 being totally overlapped by the dominant D1 component. As argued by De Grave and Van Alboom (1991), consistent results from the δ(T) curves can only be expected if a large number of very accurate experimental data are available.

As seen in Fig. 5, the variation of δ with T for the second Fe^{2+} site is much steeper than for the other Fe sites. In fact, expression (1) cannot reproduce the experimental curve with any positive value for Θ_M. The full line through the data points was calculated by tentatively introducing in (1) an additional term, linearly varying with T, and assuming Θ_M=380 K. The slope of the linear term was found to be $\approx 2.10^{-4}$ mm/s.K, i.e., one order of magnitude larger than the suggested linear variation due to the thermal expansion of the lattice (De Grave and Van Alboom 1991). The origin of this additional strong temperature dependence will be discussed in the third section of this Discussion.

Knowing at this stage the magnitudes of the Fe^{2+} and Fe^{3+} f fractions at any given temperature, the approximate composition of the sample can be indicated as:

$$Na_{1.06}Ca_{0.06}Mg_{0.04}Fe^{2+}_{0.11}Fe^{3+}_{0.90}Al_{0.06}Si_{1.91}O_6.$$

According to the earlier mentioned interpretation of the doublet MS, approximately 0.03 Fe^{3+} cations per formula unit occupy tetrahedral sites. It is likely that also the Al species substitute for Si, and hence the number of occupied Si sites in the above chemical formula totals close to the ideal value of two. However, the cation sum is unreasonably high, viz., 4.14 against the ideal value of 4.00. This finding is consistent with the detection in the XRD pattern of a small amount of an impurity phase. Whether or not this phase contains any iron could not be concluded from the present Mössbauer analyses. Therefore, it could be suggested that doublet D4 perhaps arises from ferric ions in an unidentified impurity. This doublet was introduced to avoid the need to consider an asymmetric Fe^{3+} (M1) component which cannot by justified on the basis of relaxation or texture effects. As mentioned earlier, the seemingly asymmetric ferric doublet has been observed in other aegirine samples in which presumably no impurity phase was present (Amthauer and Rossman 1984). Therefore, it seems more plausible to assign D4 to the Si sites, although its quadrupole splitting is unusually small for this type of co-ordination.

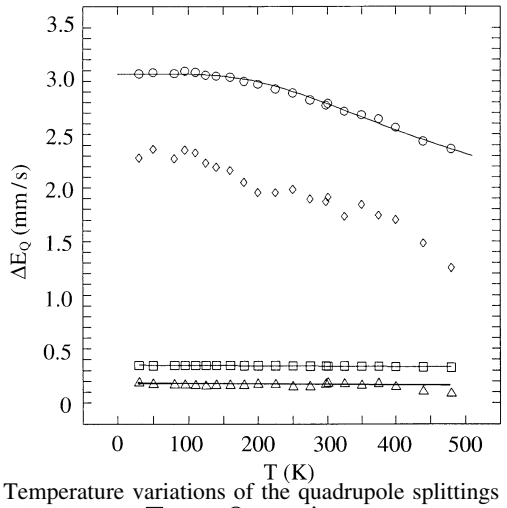

Fig. 6 Temperature variations of the quadrupole splittings ΔE_Q for the four doublets D1 (□), D2 (○), D3 (◊), and D4 (Δ) resolved from the paramagnetic spectra of aegirine. The full lines for D1 and D4 (Fe^{3+}) are the least-squares fitted straight lines. The upper curve represents the calculated variation for Fe^{2+} (M1) assuming a rhombic *case 2* point symmetry for the M1 co-ordination

Temperature variations of the quadrupole splittings

These variations are reproduced in Fig. 6 for the four distinct Fe sites. They are weak for both Fe^{3+} species and, when representing by a straight line, the slope is found to be $\approx -4.10^{-4}$ mm/s.K. This is a typical value and commonly ascribed to the expansion of the lattice with increasing T. The resulting longer inter-ionic distances give rise to a weakening of the quadrupole interactions. The extrapolated, zero-Kelvin values of 0.35 mm/s and 0.17 mm/s for Fe^{3+} (M1) and Fe^{3+} (T) respectively, are rather small, indicating that the distortions of the respective co-ordinations from their ideal symmetry are not considerable.

The interpretation of $\Delta E_Q(T)$ for Fe^{2+}-D2 was based on the point-charge model described earlier by Van Alboom et al. (1993) and successfully applied by these authors to orthopyroxenes, and more recently to riebeckite (De Grave and Van Alboom 1996). However, in the present case the theoretical treatment can only be carried out semi-quantitatively for a number of reasons, the most important ones being: (i) the effective ionic charges in aegirine have, as far as could be traced, not been determined so far; (ii) the Fe^{2+} species are impurities and, having a larger ionic radius than Fe^{3+}, the local geometry of their M1 site is likely to be different from that valid for pure aegirine, in which the M1 coordination incorporates

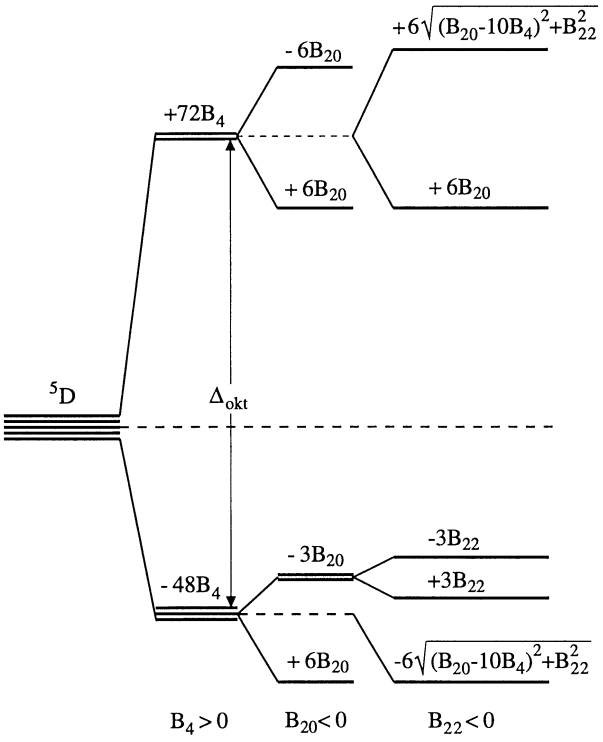

Fig. 7 Orbital energy-level scheme for the ^{5}D term of Fe^{2+} situated in a M1 site (octahedral co-ordination, $B_4\rangle 0$) with a rhombic *case 2* point symmetry. The case $B_{20}\langle 0$ corresponds to a tetragonal compression

Fe^{3+} exclusively; (iii) optical spectra for aegirine are not available so that the energy positions of the E_g electronic levels with respect to the $T_{2\,g}$ ground state are unknown.

Considering the crystallographic data reported by Cameron et al. (1973) for pure, synthetic aegirine, the rhombic *case 2* symmetry (Varret 1976b) seems to be a reasonable approximation for the real local symmetry of the M1 site. The calculations were therefore performed emanating from that approximation which, mathematically, can be treated as a perturbation on the octahedral point symmetry. Hence, the general expression of the crystal-field Hamiltonian in the point-charge model reduces to a less complicated form which in terms of Stevens' operators $\boldsymbol{O_{ij}}$, can be written as:

$$\boldsymbol{H_{r\,2}}=B_4(\boldsymbol{O_{40}}-5\,\boldsymbol{O_{44}})+B_{20}\boldsymbol{O_{20}}+B_{22}\boldsymbol{O_{22}}. \quad (2)$$

The resulting ^{5}D orbital energy-level scheme for the Fe^{2+} (M1) species is represented in Fig. 7, and, as is generally known, the magnitude of the valence contribution to the ferrous EFG at any given temperature is determined by the Boltzmann populations of the five orbital states at that temperature. The crystal-field splitting, $\Delta_{oct}=120\,B_4$, was chosen to be 8900 cm^{-1} which is close to the value found for hedenbergite (Van Alboom 1994). Considering the unavoidably approximate character of the theoretical treatment, the spin-orbit coupling was not taken into account. This simplification should not have any substantial implication for most of the other quantities incorporated in the model. Finally, the lattice contribution to the EFG was obtained from a lattice summation over a sphere with a large enough radius to produce convergence.

Under the above specified conditions and approximations, the coefficients B_{20} and B_{22} were found to be -145 cm^{-1} and -265 cm^{-1} respectively, yielding for the energy positions of the four excited ^{5}D levels respectively 590, 2170, 8970, and 10780, all in cm^{-1} and with respect to the ground state. The presently determined energy gaps for the first two excited states are broader as compared to other pyroxene materials (Van Alboom et al. 1993; Van Alboom 1994). This finding might point at a stronger distortion of the Fe^{2+}-containing M1 sites in aegirine. The calculated temperature variation of the quadrupole splitting is plotted as a full line in Fig. 6, and reproduces the experimental curve reasonably well. The quadrupole-coupling constant ΔE_0 was fitted as 3.47 mm/s from which the covalence factor, usually symbolised as α^2_{cov}, is calculated to be 0.92. The lattice contribution was found to be -0.36 mm/s. The remarkable agreement of this latter value with the observed Fe^{3+} (M1) quadrupole splitting is believed to be merely fortuitous. Finally, the asymmetry parameter η of the total EFG was calculated at any given temperature. The values came out small (0.12 at 80 K), but are underestimated as a result of neglecting the spin-orbit coupling.

The experimental $\Delta E_Q(T)$ curve for Fe^{2+}-D3 exhibits significant scatter and unreal, sudden changes in the local slope. No further attempts have been undertaken to relate this observed dependence to structural characteristics of the mineral. Considering the nature of this doublet (see next section), this would present little physical meaning after all. It is interesting to note, though, that the splittings of this doublet are consistently and considerably smaller than those derived for the other Fe^{2+} site, although both have the M1 co-ordination.

Nature of the Fe^{2+}-D3 component

As mentioned in the introduction, Amthauer and Rossman (1984) interpreted their observations concerning the Mössbauer parameters of the two Fe^{2+} doublets in terms of a thermally activated electron-hopping process involving pairs of Fe^{2+}–Fe^{3+} cations on adjacent M1 sites. This would indeed account for the otherwise unexplainable lowering of δ of doublet D3 as T increases, and for the increase of its fractional contribution S at the expense of that of doublet D2. If this phenomenon indeed takes place, one might raise the question why a comparable decrease in the S value of the Fe^{3+} (M1) doublet is not observed. Referring to Table 1, this latter S value remains more or less constant, whereas one would expect to find a small but statistically significant lowering on going to higher temperatures. However, this reasoning is incorrect since it does not take into account that the Mössbauer fraction f_2 of the Fe^{2+} species is smaller than that of the Fe^{3+} species (f_3), the differences becoming more pronounced at higher T. Considering the area fractions S_i (i=D1,..., D4) obtained at 80 K (see Table 1), and the

Mössbauer fractions f_2 and f_3 as specified earlier, and assuming hypothetically that no changes in the valence states of any of the Fe species occur, then one expects at 480 K to observe S_i values of 0.87, 0.06, 0,03, and 0.04 for D1 to D4 respectively. The data of Table 1 hence show that possibly ∼0.03 of each of the Fe^{3+} (M1) and Fe^{2+} (M1) sites per formula unit, have been converted to the earlier denoted Fe^{2+} (M1)-D3 species on going from 80 K to 480 K. Considering the estimated area errors, this number of 0.03 cations might appear as being of little significance, but, it is nonetheless in line with the suggestion of an electron-exchange process on a time scale comparable to or smaller than that for the γ-absorption process. Consequently, the hyperfine interactions experienced by the Mössbauer effect are time-averaged interactions, thus yielding hyperfine-parameter values in between those of the static Fe^{3+} (M1) and Fe^{2+} (M1) species. The apparent valence of the exchanging pairs of Fe ions, and hence their observed hyperfine parameters, depend on the relaxation rate of the hopping process, and it is conceivable that for a given sample this rate fluctuates due to variations in next-nearest neighbour cation configurations and compositional heterogeneities, the more so at higher temperatures at which there is a higher degree of delocalization of electrons. This would explain the observed increase of the line width of the corresponding doublet with increasing T, in this case from 0.41 mm/s at 30 K to 1.05 mm/s at 480 K.

Further consideration of the various assumptions on which the qualitative model of thermally activated electron exchange is based, suggests that this model is not entirely satisfactory in the case of aegirine. At temperatures as low as 30 K the exchange process is thought to be frozen-in. Yet, the Fe^{2+} ions occupy two distinct M1 sites characterised by nearly equal centre shifts, but with a difference of ≈0.8 mm/s in their quadrupole splittings. This implies that at low temperatures the orbital configuration states of the respective ferrous species are significantly distinct due to, e.g., different distortions of the M1 co-ordination, the less distorted site giving rise to the outer ferrous doublet. The proposed electron-exchange process as observed from the MS at higher temperatures would then involve one Fe^{3+} (M1) site and two different Fe^{2+} (M1) sites simultaneously, which is difficult to conceive.

An alternative explanation of the observed temperature variation of the Mössbauer parameters may be that part of the ferrous ions flip from one configuration to the other as the temperature changes. This phenomenon in similar clinopyroxenes has been considered earlier by Dollase and Gustafson (1982) and these authors suggested that the existence of two (or a multitude of) possible electronic configurations might result from different short-range chemical environments of the iron species. They further theorised that the temperature at which a given probe Fe^{2+} ion changes its orbital state depends on the sum of all its atomic interactions with neighbouring species, so that the population of the least distorted state increases gradually with increasing temperature. This would imply that the range of different high-temperature orbital configurations broadens with temperature, and also could explain the appearance of an additional temperature dependence of the measured average centre shift, which is sensitive to the chemical bond of the probe Fe^{2+} to its environment.

In summary, two distinct mechanisms seem to be able to explain the multiple ferrous doublets associated with the same crystallographic sites in this studied aegirine sample. Both of them raise some questions which should trigger further experimental endeavours. The first model would require a rather unusual path for the transfer of charge between one Fe^{3+} (M1) and one Fe^{2+} (M1) on the one hand, and a second distinct Fe^{2+} (M1) on the other hand. Concerning the second model, it remains unclear why the occurrence of distinct electronic configurations for Fe^{2+} in the same crystallographic site, and the gradual thermally induced transformation between them, seems to be restricted to Ca–Na clinopyroxenes (Dollase and Gustafson 1982).

Magnetic hyperfine-field distributions

As indicated in a previous section, the appearance of the low-temperature (4.2 K) MS of the investigated aegirine mineral suggests a broad distribution in hyperfine fields and the spectral shape could satisfactorily be reproduced as such. The principal source of this distribution was attributed to fluctuations in the chemical and structural environment of the probe iron nuclei. In second order, the non-unique angle between the field direction and the EFG principal axis also contributes to the broadening of the line shape. The presence of compositional and/or structural heterogeneities has two implications on the magnetic hyperfine fields. First, it gives rise to fluctuations in the saturation hyperfine field and in the magnetic exchange interactions. These latter fluctuations produce considerable field distributions, the more so at more elevated reduced temperatures T/T_N (De Grave et al. 1988).

Secondly, the aforementioned fluctuations may result in a range of transition temperatures T_N at which three-dimensional magnetic ordering starts to develop according to the Mössbauer observation. The consequence of this is that at T=4.2 K (or any other temperature in the magnetically ordered state) the reduced temperature T/T_N, and hence the magnitude of the hyperfine field, are spread out over a finite range of continuously varying values. This feature seems to be relevant in the case of aegirine. Baum et al. (1988) report a MS recorded for a synthetic single-crystal of $NaFeSi_2O_6$ at 10 K. The spectrum clearly consists of a part that is magnetically ordered and a part that is not. Hence, the sample obviously has no unique transition temperature T_N. A similar superposition was observed by Ballet et al. (1989), also for a synthetic sample.

Baum et al. (1988) further claimed that the slightly asymmetric line broadening of their magnetic subspectrum at 10 K was due to relaxation effects. Solid evidence to corroborate this suggestion was not given in their paper. There are two capital arguments that such effects play

an insignificant role with respect to the line shape of the MS shown in Fig. 3. First, this line shape is well reproduced on the basis of static hyperfine fields, which means that the peak velocities of each given sextet component are a linear function of the magnitude of the corresponding hyperfine-field value. Such a linear relation is not applicable in case of relaxation MS (Wegener 1965, 1975) and hence, these spectra cannot be described in a manner as used in this work.

Secondly, the response of the magnetic structure of the investigated aegirine sample to the application of an external magnetic field (Fig. 4) is typical for a powder exhibiting a static antiferromagnetic ordering (De Grave et al. 1992). In case of spin relaxation the external field will affect the relaxation rate which is expected to be reflected in the MS in a way depending on the nature of the relaxation mechanism, but certainly different from what is observed in the applied-field MS presented in this paper.

Conclusions

Two important structural implications have emerged from this detailed set of measurements and their analyses: (i) the possible presence of a small amount of Fe^{3+} in the Si sites, thus explaining the asymmetric peak depths of the ferric component and ruling-out the (unlikely) suggestion of the presence of relaxation effects at high temperatures; (ii) the confirmation of the occurrence of Fe^{2+} on two distinct M1 sites and the gradual, thermally induced change in the populations of these sites; two different models to explain this feature have been discussed, viz., intervalence charge transfer and the formation in the structure of two predominant orbital configurations for the Fe^{2+} species, the first configuration being favoured at low temperatures, the second one at higher temperatures.

The interpretation of the temperature variations of the Fe^{3+} (M1) and Fe^{2+} (M1) centre shifts has again confirmed that in a given lattice, the Mössbauer fraction for ferrous ions is smaller than that for ferric ions. The calculated lattice temperatures Θ_M are consistent with the values reported earlier for a number of different silicates. The observed quadrupole splittings indicate that the M1 polyhedra containing Fe^{3+} cations are only slightly distorted, in contrast to those containing Fe^{2+}.

At 4.2 K the sample studied is magnetically ordered. The shape of the external-field spectrum at that temperature is consistent with a static antiferromagnetic spin structure. The importance at 4.2 K of relaxation effects was concluded to be insignificant. Both the Fe^{2+} and Fe^{3+} hyperfine fields extend over a broad range of values, with maximum-probability fields of 467 kOe and 220 kOe respectively. The field distributions are thought to be due to spatial fluctuations in the chemical compositions of the near-neighbour shells of the probe iron nuclei.

Acknowledgements This work was supported by the Fund of Joint Basic Research, Belgium.

References

Akasaka M (1983) ^{57}Fe Mössbauer study of clinopyroxenes in the join $CaFe^{3+}AlSiO_6$–$CaTiAl_2O_6$. Phys Chem Minerals 9:205–211

Amthauer G (1982) Gemischte Valenzzustände des Eisens in Mineralen. Fortschr Mineral 2:119–154

Amthauer G, Rossman GR (1984) Mixed valence of iron in minerals with cation clusters. Phys Chem Minerals 11:37–51

Annersten H, Nyambok IO (1978) Iron distribution in aegirine-augite clinopyroxenes studied by Mössbauer effect. University of Uppsala, Department of Mineralogy and Petrology, Research Report No. 11, Uppsala

Ballet O, Coey JMD, Fillion G, Ghose A, Hewat A, Regnard JR (1989) Magnetic order in acmite; $NaFeSi_2O_6$. Phys Chem Minerals 16:672–677

Baum E, Treutman W, Behruzi M, Lottermoser W, Amthauer G (1988) Structural and magnetic properties of the clinopyroxenes $NaFeSi_2O_6$ and $LiFeSi_2O_6$. Z Kristallogr 183:273–284

Cameron M, Papike JJ (1980) Crystal chemistry of silicate pyroxenes. In: Prewitt CT (ed) Pyroxenes (Reviews in Mineralogy vol. 7). Mineralogical Society of America, Washington DC, pp 5–92

Cameron M, Sueno S, Prewitt CT, Papike JJ (1973) High-temperature crystal chemistry of acmite, diopside, hedenbergite, jadeite, spodumene and ureyite. Am Mineral 58:594–618

Chambaere D, De Grave E (1984) On the Néel temperature of β-FeOOH: structural dependence and its implications. J Magn Magn Mater 42:263–268

Collins RL, Travis JC (1967) The electric field gradient tensor. In: Gruverman IJ (ed) Mössbauer effect methodology, vol. 3. Plenum, New York, pp 123–161

de Bakker PMA, De Grave E, Persoons RM, Bowen LH, Vandenberghe RE (1990) An improved, two-parameter distribution method for the description of the Mössbauer spectra of magnetic small particles in an applied field. Meas Sci Technol 1:954–964

Deer WA, Howie RA, Zussman J (1978) Rock forming minerals, vol. 2A: Single chain silicates (2nd edn). Longman, London

De Grave E, Van Alboom A (1991) Evaluation of ferrous and ferric Mössbauer fractions. Phys Chem Minerals 18:337–342

De Grave E, Van Alboom A (1996) Temperature dependence of the ^{57}Fe Mössbauer parameters in riebeckite. Phys Chem Minerals 23:377–386

De Grave E, Bowen LH, Amarasiriwardena DD, Vandenberghe RE (1988) ^{57}Fe Mössbauer effect study of highly substituted aluminum hematites: determination of the magnetic hyperfine field distributions. J Magn Magn Mater 72:129–140

De Grave E, de Bakker PMA, Bowen LH, Vandenberghe RE (1992) Effect of crystallinity and Al substitution on the applied-field Mössbauer spectra of iron oxides and oxyhydroxides. Z Pflanzenernähr Bodenk 155:467–472

de Oliveira JCP, da Costa MI, Schreiner WH, Vasquez A, Veivia N, Roisenberg A (1988) Magnetic order in acmite: $Ac_{81}Di_{19}$. J Magn Magn Mater 75:171–174

Dollase WA, Gustafson WI (1982) ^{57}Fe Mössbauer spectral analysis of the sodic clinopyroxenes. Am Mineral 67:311–327

Heberle J (1971) The Debye integrals, the thermal shift and the Mössbauer fraction. In: Gruverman IJ (ed) Mössbauer effect methodology, vol. 7. Plenum, New York, pp 299–308

Johnson CE (1967) Hyperfine interactions in ferrous fluosilicate. Proc Phys Soc London 92:748–757

Le Caër G, Dubois JM, Fisher H, Gonser U, Wagner HG (1984) On the validity of ^{57}Fe hyperfine field distribution calculation from Mössbauer spectra of magnetic amorphous alloys. Nucl Instrum Methods B5:25–33

Morimoto N (1988) Nomenclature of pyroxenes. Am Mineral 73:1123–1133

Nagy DL (1978) Deformation-induced texture in Mössbauer absorbers. Appl Phys 17:269–274

Sawatzky GA, van der Woude F, Morrish AH (1969) Mössbauer study of several ferrimagnetic spinels. Phys Rev 187:747–757

Tröger WE (1952) Tabellen zur optischen Bestimmung der gesteinsbildenden Minerale. Schweizerbart'sche Verlag, Stuttgart

Van Alboom A (1994) Studie van de temperatuurafhankelijkheid van de ^{57}Fe-mössbauerparameters in ijzerhoudende silicaten. PhD thesis, University of Gent

Van Alboom A, De Grave E, Vandenberghe RE (1993) Study of the temperature dependence of the hyperfine parameters in two orthopyroxenes by ^{57}Fe Mössbauer spectroscopy. Phys Chem Minerals 20:263–275

Vandenberghe RE, De Grave E, de Bakker PMA (1994) On the methodology of the analysis of Mössbauer spectra. Hyperfine Interact 83:29–49

Varret F (1976a) Mössbauer spectra of paramagnetic powders under applied field: Fe^{3+} in fluosilicates. J Phys Chem Solids 37:265–271

Varret F (1976b) Crystal-field effects on high-spin ferrous iron. J Phys Colloq 37:C6 437–456.

Wegener HHF (1965) Über die Hyperfeinstrukturaufspaltung der Mößbauerstrahlung durch zeitlich fluktuierende Magnetfelder. Z Phys 186:498–511

Wegener HHF (1975) The study of relaxation mechanisms by means of the Mössbauer spectroscopy. In: Hrynckiewicz AZ, Sawicki JA (eds) Proceedings International Conference on Mössbauer Spectroscopy, vol. 2, Akademia Górniczo-Hutnicza, Krakowie, pp 257–274

Wickman HH, Wertheim GK (1968) Spin relaxation in solids and aftereffects of nuclear transformations. In: Goldanskii VI, Herber RH (eds) Chemical Applications of Mössbauer spectroscopy. Academic Press, New York, pp 548–621